

Short Communication

Evaluation of the Weld on In-service Gas Pipeline

Mária Mihalikova¹, Mária Hagarova¹, Dagmar Jakubéczyová², Jana Cervová^{1,*}, Anna Lišková¹

¹Department of Materials Science, Faculty of Metallurgy, Technical University of Košice, Slovakia

²Institute of Materials Research, Slovak Academy of Sciences, Košice, Slovakia

*E-mail: jana.cervova@tuke.sk

Received: 28 January 2016 / Accepted: 29 March 2016 / Published: 4 May 2016

The study evaluated the condition of steel gas pipeline at the site of weld after more than 45 years of service. The deformation cycle of welding and particularly superposition of the thermal and deformation cycle, results in phase transformation and precipitation processes in the thermally affected region. The deformation cycle has a pronounced effect on ageing of the welded joint and the associated increase in its hardness and reduction in notch toughness. The hardness of the weld was measured according to Vickers HV0.05. The highest values of hardness were measured for the weld metal, namely 293 HV0.05. The values of mechanical properties of steel after more than 45 years of service of the pipeline corresponded to values defined by the respective standard. Transition temperature T_T according to Charpy test was equal to -8.5 °C. From the point of view of technical practice, with regard to pipe service properties, it is important that the construction material is loaded at temperatures above the transition temperature T_T . Transcrystalline brittle failure was observed on the specimens that have been broken at T_T temperature.

Keywords: gas pipeline, steel, welded joint, transition temperature, fracture

1. INTRODUCTION

The gas pipeline represents potential risk related to operational pressure, mechanical stress (landslides, excavation) and corrosion degradation [1,2]. Welded joints are critical sites of steel gas pipelines due to their construction under external conditions during pipeline laying. In addition to climate conditions, there are other important factors, such as the pipeline material, the way of laying down, welding technology and quality of the welded joints. The steel pipeline are the most commonly exposed in soil environment which can cause the corrosion attack. The corrosion process of outer surface of gas pipeline acquires an electrochemical character dependent on character soil, chemical composition of soil electrolyte, presence of microorganisms and other. Electrochemical character take place according to following equations [3,4]



Manual metal arc welding belongs among the most frequently used technologies of welding of steel gas pipe systems. Welding results in changes in material properties in the thermally affected region. These changes involve particularly the structure and substructure of steel but also precipitation processes [5-8]. In addition, distribution and density of dislocations in steel are affected and thus also the plasticity of steel. Moreover, the changes in distribution of contaminants affect essentially the welded joint properties. On the basis of knowledge of the mechanism and kinetics of these changes, it is possible to envisage in detail the expected properties of thermally affected regions. However, the majority of welded joints are systems which comprise, besides the thermally affected region, also the weld metal with its structural, substructural and dislocation aspects. The plasticity of heat affected zone same as weld metal are harder to control. Therefore these regions have become a weak link in pipelines. The basic phases that can be considered in welded steel pipeline are ferrite, pearlite, martensite and austenite. Other phases such as sorbide, bainite. The most commonly observed microstructure in the weld deposit of low carbon steel is acicular ferrite [9-11]. Despite the increasing use of microalloyed steels or steels with sufficiently low content of nitrogen in welded constructions, complications related to ageing of welded joints still occur relatively frequently. Ageing of steels is related to re-distribution of atoms of interstitial nitrogen and partially also of carbon in αFe . If the concentration of nitrogen in steel exceeds 0.003 %, rapid cooling of steel from the temperature of Ac1 may result in the development of over-saturated solid solution susceptible to ageing. During such ageing changes in physical and mechanical properties of steel occur reflected in increased hardness, yield point and deterioration of plastic properties. The most negative consequence in the thermally affected ageing region in welded steels is the pronounced reduction in notch toughness [12].

2. EXPERIMENTAL MATERIAL AND METHODS

The weld on the steel P295 GH gas pipeline after more than 45 years in service was evaluated by means of a light microscope OLYMPUS VANOX-T. The metallographic analysis was used as a tool to help to identify uniform structure of steel pipeline. The sampling points are illustrated in Figure 1. The strength properties and plasticity of the steel gas pipeline were evaluated by means of a tensile test according to EN ISO 6892-1 at ambient temperature $T = 20 \pm 3 \text{ }^\circ\text{C}$, employing a tensile test machine ZWICK 1387 at loading $0 \div 200 \text{ kN}$ and speed $1 \text{ mm}\cdot\text{min}^{-1}$ [13]. Mechanical properties (yield point $R_{p0.2}$, tensile strength R_m and ductility A_5) of P295 GH steel were determined on circular section specimens of dimensions $d_0 = 5 \text{ mm}$ and $L_0 = 10 \text{ mm}$, removed from the gas pipe in a direction parallel to the longitudinal axis of the pipe, and in direction transversal to the pipe axis. Microhardness

HV0.05 of the weld was determined according to ISO 5817 in the weld region according to Figure 2 [14].

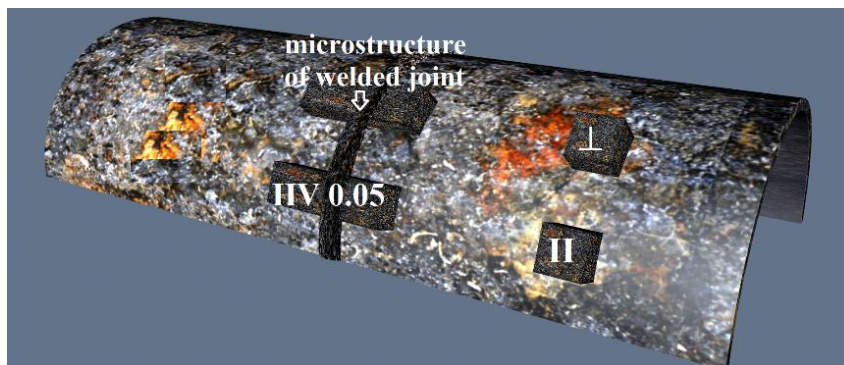


Figure 1. Sampling points

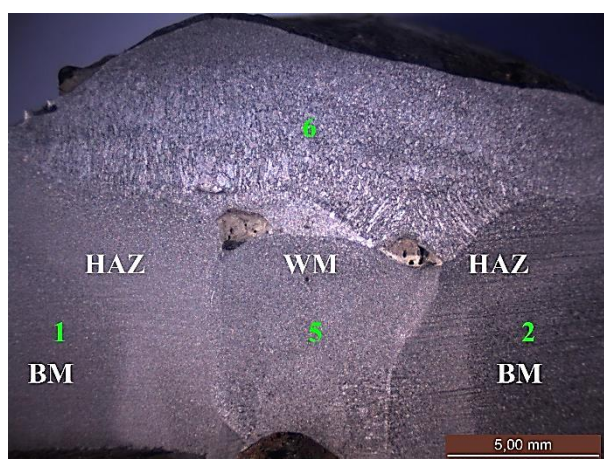


Figure 2. Weld on the pipeline steel with HV0.05 hardness measurement in points 1,2,5,6

The effect of temperature of transit behaviour of structural materials is most commonly determined by Charpy test. The samples with dimension 55 x 10 x 5 mm and V notch of 2 mm were broken by means Charpy hammer in the temperature range from $-60\text{ }^{\circ}\text{C}$ to $+20\text{ }^{\circ}\text{C}$. To obtain the required temperature the samples were placed in a cooling chamber of liquid nitrogen. The V notch test was carried out on a test machine ZWICK 1387, the parameters of which corresponded to the standard EN 10045-2. Such test consists in the breakage of a test rod notched in the centre and supported at both ends by one strike of a pendulum, under the conditions defined by standards EN 10045-1 and EN 10045-2 [15-17]. For determination of transition temperature, the standard EN ISO 148-1 sets the criterion of impact energy $K = 27\text{ J}$ [18]. The fracture surface of steel specimens after the Charpy test was analyzed by means of scanning electron microscope JEOL JSM-7000F. The fractographic analysis included also EDX analysis by a micro-analyser INCAx_sight. Chemical composition of the welded steel is presented in Table 1.

Table 1. Chemical composition of steel P295GH

Chemical composition in wt. %							
Element	C	Si	Mn	P	S	Al	N
	0.2	0.44	0.93	0.03	0.025	0.020	0.006

3. RESULTS AND DISCUSSION

The structure of P295GH steel (basic material – BM) is documented in Figure 3 and Figure 4. The microstructure of steel parallel to the longitudinal axis of the pipeline was ferrite – pearlite and showed a pronounced line-like structure in ferrite and pearlite, see Figure 3.

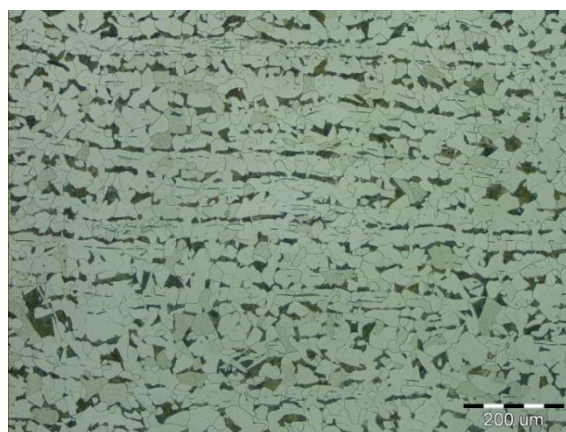


Figure 3. Microstructure of steel parallel to the longitudinal axis of the pipeline, etch. Nital

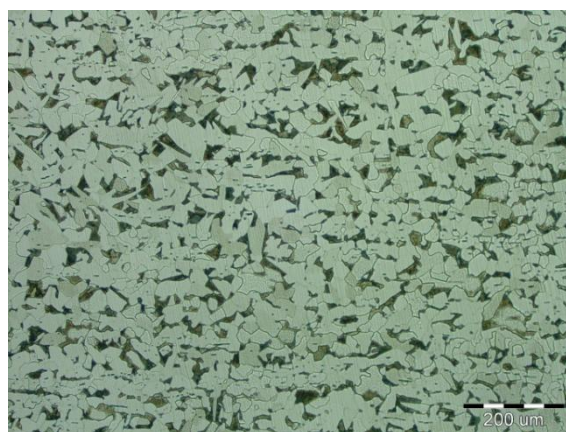


Figure 4. Microstructure of steel transversal to pipeline axis, etch. Nital

Sulphidic inclusions were observed in the microstructure. The microstructure of steel oriented transversally to pipeline axis, see Figure 4, was similar to steel parallel to the direction of rolling except for the inclusions which were considerably shorter. The occurrence of inclusions in non-etched steel is illustrated in Figure 5 and Figure 6. The microstructure of the weld metal (WM), Figure 7,

consisted of coarse acicular ferrite with Widmanstätten pattern and pro-eutectoid ferrite. The microstructure of heat affected zone (HAZ), Figure 8, was composed of acicular ferrite and polyhedral ferrite.

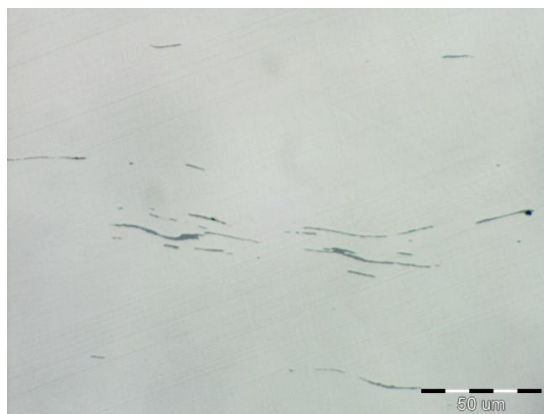


Figure 5. Occurrence of inclusions elongated in the direction of rolling, non-etched

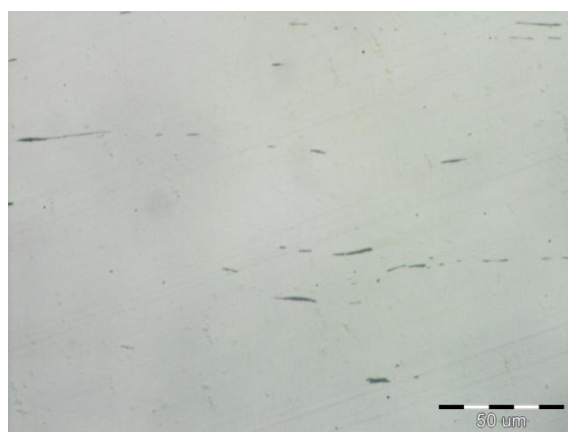


Figure 6. Occurrence of inclusions oriented perpendicularly to rolling, non-etched



Figure 7. Microstructure of weld metal, etch. Nital

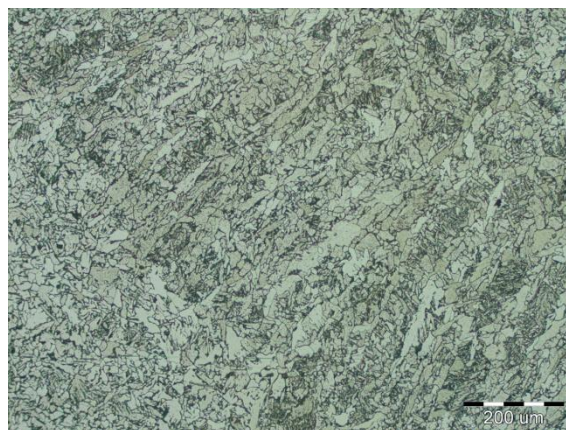


Figure 8. Microstructure of thermally affected region, etch. Nital

The values of microhardness HV0.05 of the weld are presented in Table 2 and are reported as means of three measurements obtained at sites according to Figure 2.

Table 2. Values of microhardness HV0.05 of welded joint

Site of measurement	HV0.05 microhardness
1	201
2	192
3	270
4	203
5	219
6	293

The highest values of hardness were measured for the weld metal, namely 293 HV0.05. The lowest values of hardness were measured in the region of the welded material with ferritic – pearlitic structure, namely 192 HV0.05. Results of measurements of mechanical properties of the steel gas pipeline are presented in Table 3 and compared with values set by EN 10028/2-92 [19]. The values of yield point and tensile strength for both orientations of sampling after more than 45 years of service of the pipeline corresponded to values defined by the respective standard.

Table 3. Mechanical characteristics of steel

Specimen	R _{p0.2} (MPa)	R _m (MPa)	A ₅ (%)
Parallel to the direction of rolling	275	464	27.6
Perpendicular to pipeline longitudinal axis	280	465	33.0
According to EN 10028/2-92	295	460-580	min 22.0

The values of impact energy obtained by the V notch test are presented in Table 4. The value of the impact energy is defined as K = 27 J, as stated by the standard STN EN ISO 148-1 for the

determination of transition temperature T_T [18]. Figure 9 shows the thermal relationship for the impact energy and the obtained transition temperature, which in our case was equal to $T_T = -8.5^\circ\text{C}$. From the point of view of technical practice, with regard to pipe service properties, it is important that the construction material is loaded at temperatures above the transition temperature T_T .

Table 4. Results of V notch test

Temperature ($^\circ\text{C}$)	+20			0			-10		
Energy (J)	68	71	74	43	42	47	18	17	17,5
Temperature ($^\circ\text{C}$)	-20			-40			-60		
Energy (J)	16	15.6	14.3	12.4	11.9	11	10	8	10

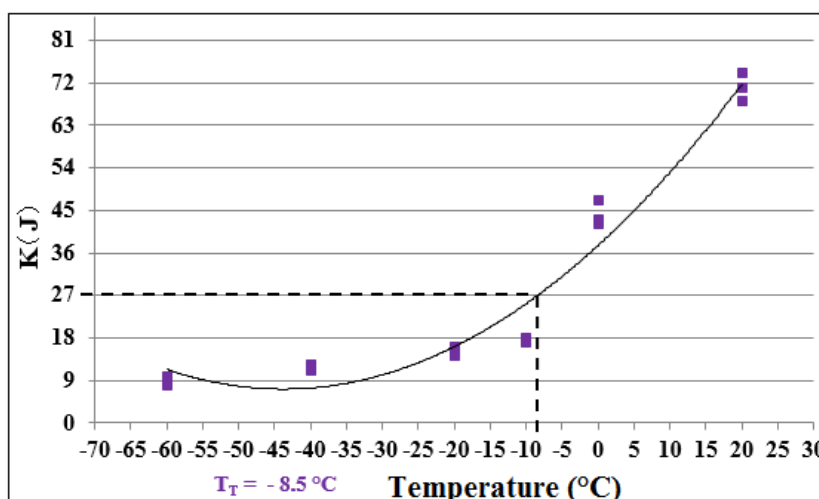


Figure 9. Thermal relationship for the impact energy K and the transition temperature obtained from the curve; $T_T = -8.5^\circ\text{C}$ at $K = 27$ J

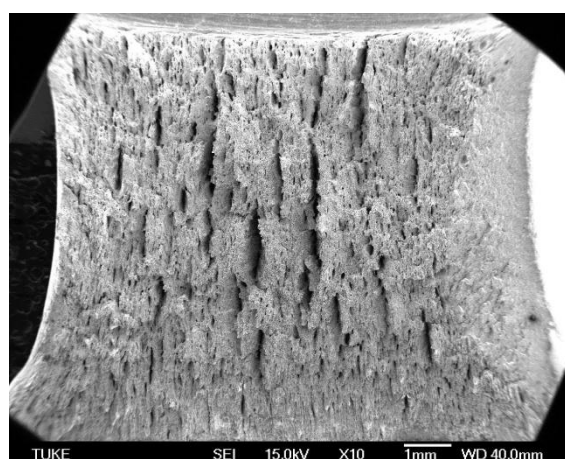


Figure 10. Fracture surface of a specimen fractured at temperature $+20^\circ\text{C}$, SEM

The macroscopic pictures of fracture surfaces of specimens obtained by the Charpy test at temperatures -10°C , 0°C and $+20^\circ\text{C}$ are shown in Figures 10, 14 and 18. For evaluation of fracture

surfaces, we selected specimens fractured at temperatures close to the determined transition temperature. The macroscopic examination of specimen surface presented in Figure 10 showed that transcrystalline plastic failure with pitted morphology was predominantly involved.

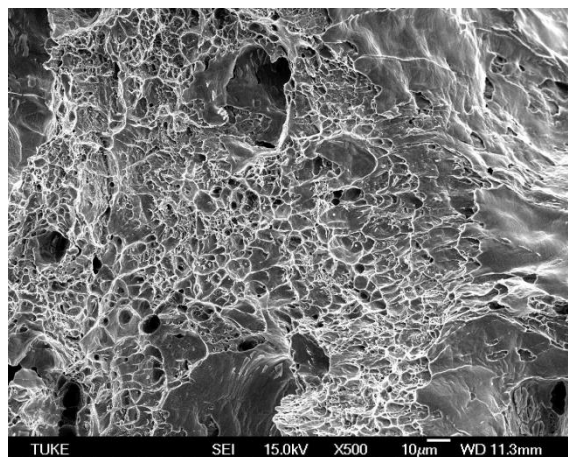


Figure 11. Transcrystalline plastic failure with pitted morphology, SEM

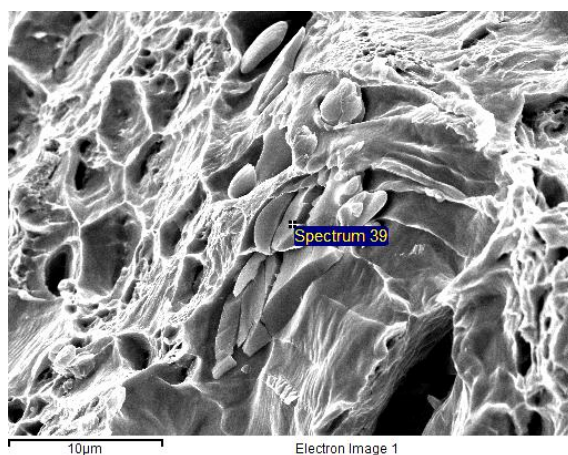


Figure 12. Inclusions in fracture pits, SEM

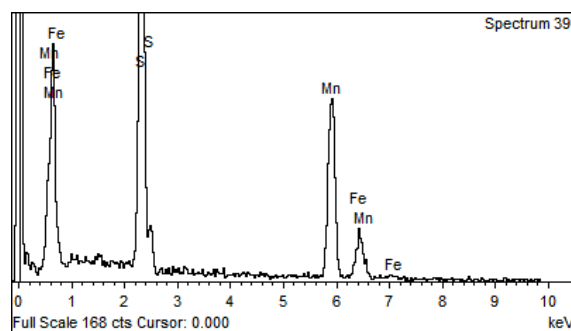


Figure 13. EDX analysis of inclusion depicted in Figure 12, SEM

The fracture surface in Figure 10 is rough with ridges and specimen edges show signs of plastic deformation. Pronounced lines of elongated pits oriented parallel to the surface of the steel pipe are visible in fracture morphology. Details of these elongated pits initiated by rolled inclusions present in the steel are shown in Figures 11 and 12. The size of the pits which developed by plastic failure of the respective specimen and were initiated by inclusion particles in respective specimens differs. In large pits one can observe relatively large inclusion particles (Figure 12). EDX analysis of such particle, as documented in Figure 13, showed presence of S and Mn and eventually of Fe. This involves either sulphide MnS, or complex sulphide MnFeS particles.

The fracture surface of a specimen documented in Figure 14 shows the mostly presence of cleavage facets of transcrystalline brittle failure. The fracture surface is less rough and specimen edges do not show considerable deformation. Pronounced lines of elongated pits oriented parallel to steel surface are visible in fracture morphology.

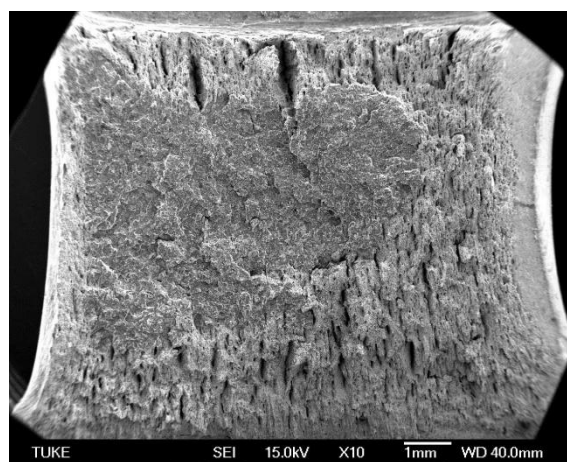


Figure 14. Fracture surface of a specimen fractured at 0 °C, SEM

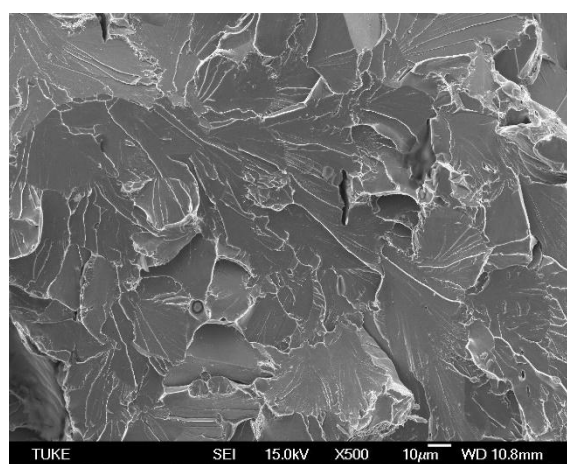


Figure 15. Transcrystalline cleavage failure of the specimen, SEM

The specimen edges are slightly rounded which indicates an increased degree of plastic deformation of steel in this region, introduced by bending impact test. Details of morphology of

transcrystalline brittle failure of fracture surface depicted in Figure 14 are documented in Figures 15 and 16. The morphology consists of transcrystalline cleavage facets locally separated by elevated levels (see detail in Figure 16). Among cleavage facets one can also observe regions of intercrystalline brittle separation of grains. The presence of intercrystalline facets provides the proof of the intercrystalline brittleness of ferrite induced as a rule by segregation of atoms of contaminants, such as P and S.

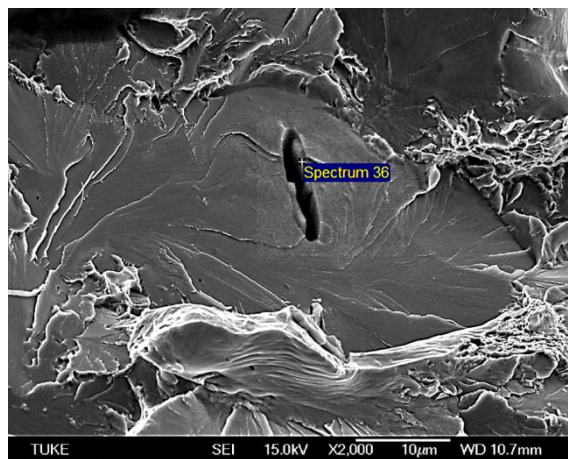


Figure 16. Inclusions in a cleavage facet, SEM

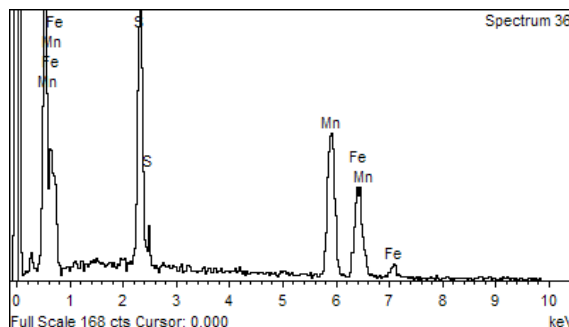


Figure 17. EDX analysis of inclusion depicted in Figure 16.

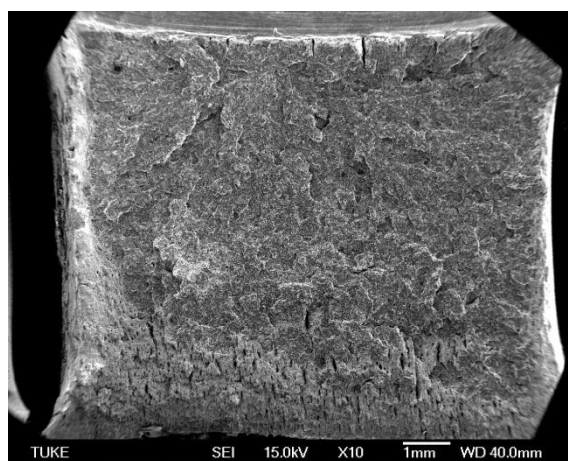


Figure 18. Fracture surface of a specimen fractured at -10 °C, SEM

This assumption is confirmed by the presence of inclusion particles (sulphides) close to this region with intercrystalline facets (marked inclusion in Figure 16). EDX analysis of this particle, with its spectrum presented in Figure 17, confirms the presence of sulphide particles in the structure of steel.

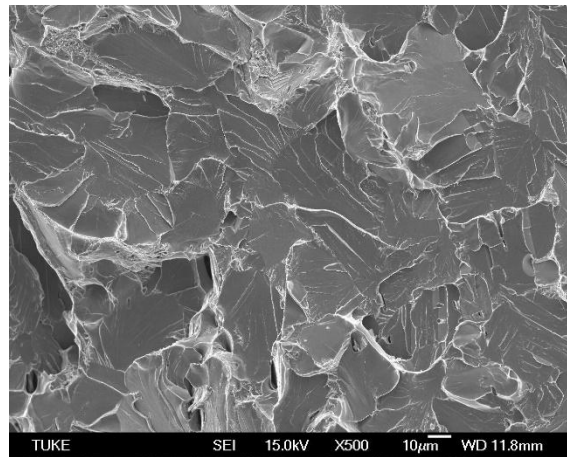


Figure 19. Transcrystalline brittle failure of the specimen, SEM

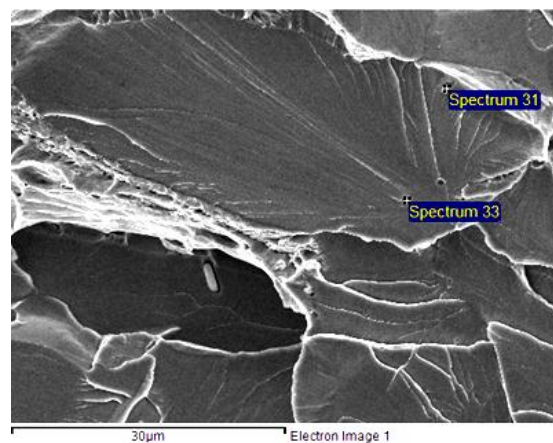


Figure 20. Detail of the region of intercrystalline brittle failure on fracture surface, SEM

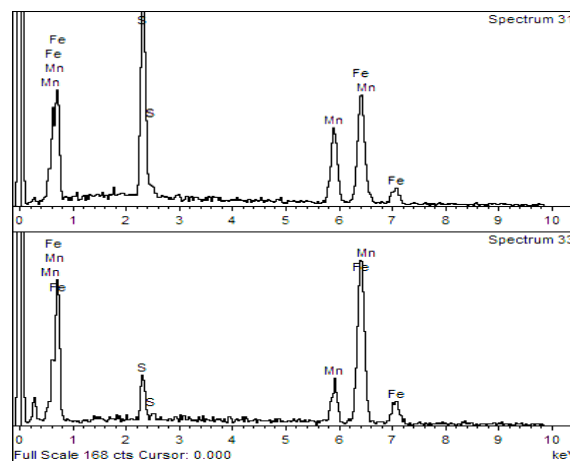


Figure 21. EDX analysis of inclusions, SEM

The majority of the fracture surface of the specimen fractured at $-10\text{ }^{\circ}\text{C}$, as shown in Figure 18, consisted of facets of transcrystalline brittle failure. The fracture surface is relatively flat and specimen edges are less deformed than those of specimens depicted in Figures 10 and 14. In the lower part of the specimen one can see a region of transcrystalline plastic failure, which takes up a small proportion of the area of fracture surface. It consisted of transcrystalline cleavage facets separated by elevated levels of varying size.

4. CONCLUSION

Evaluation of the weld on steel gas pipeline after 45 years in service showed the following:

1. The structure of the pipeline steel (welded material in our case) was ferrite – pearlite, with pronounced line-like structure in both ferrite and pearlite. This steel is determined according to the steel producer.

2. Under the influence of temperature during the welding, the properties of the heat affected zone (HAZ) changed due to structural and substructural changes; the microstructure of HAZ was composed of acicular ferrite and polyhedral ferrite.

3. Measurements of hardness HV0.05 showed that the weld metal, which consisted of coarse acicular ferrite and pro-eutectoid ferrite, reached the highest hardness of 293 HV0.05. The hardness of the welded material reached 192 HVO.05.

4. Charpy test was used to determine transition temperature T_T according to the criterion of the value of impact energy $K = 27\text{ J}$, and was equal to $-8.5\text{ }^{\circ}\text{C}$. In the technical practice, with regard to service properties, it is important to expose the constructional material to the load at temperatures exceeding T_T . According to the data provided by the pipeline operator, the lowest mean in-service operation temperature of the pipeline was $7\text{ }^{\circ}\text{C}$.

5. The values of mechanical properties for both orientations of sampling after more than 45 years of service of the pipeline corresponded to values defined by the respective standard. The yield point of steel reached the values from 275 to 280 MPa, the values of tensile strength had from 464 to 465 MPa and ductility was from 27.6 to 33.0 %.

6. Macroscopic observation and fractographic evaluation of the fracture surface of specimens following the notch toughness test (at $0\text{ }^{\circ}\text{C}$ and $-10\text{ }^{\circ}\text{C}$) showed a relatively high proportion of transcrystalline cleavage. Among cleavage facets we observed also regions of intercrystalline brittle separation. The intercrystalline facets are a proof of the intercrystalline brittleness of ferrite, caused by segregation of contaminants at ferrite boundaries, what define the character of embrittlement of steel. The morphology of inclusions observed on the fracture surface resulted from reshaping of inclusions in the direction of rolling and negatively affected the toughness, strength and plasticity of the investigated steel.

7. The inclusion particles elongated in the direction of the longitudinal pipe axis could contribute to reduced ductility A_5 in the direction perpendicular to the longitudinal pipe axis.

ACKNOWLEDGEMENTS

This study was supported by the Grant Agency of Slovak Republic, grant project VEGA 1/0549/14 and grant project VEGA 2/0061/14.

References

1. M. A. Bodude, S.O. Adeousun, W.A. Azoola. Comparative Studies On Mechanical and Corrosion Characteristics of API 5L X60 Steel and RST 37-2 Steel, *Journal of Emerging Trends in Engineering and Applied Sciences (JETEAS)*. 3, 1 (2012) 137-143
2. I. S. Cole, D. Marney. The science of pipe corrosion: A review of the literature on the corrosion of ferrous metals in soils, *Corrosion Science*. 56, 0 (2012) 5-16
3. QI Beimeng, C. Chongwei and Y. Yixing, *Int. J. Electrochem. Sci.*, 10 (2015) 545 – 558
4. J. Cervová, M. Hagarová *Acta Metallurgica Slovaca*, Vol. 21, 2015, No. 2, p. 102-110
5. V. Petrescu, G. Paraschiv, and D. Dobrota, *Metalurgija*, 55 (2016) 2.
6. Y. Yang, L. Shi, Z. Xu, H. Lu, X. Chen and X. Wang, *Engineering Fracture Mechanics*, 148 (2015) 337-349.
7. X. Chen, H. Lu, G. Chen and X. Wang, *Engineering Fracture Mechanics*, 148 (2015) 110-121.
8. H.K. Sung, S.Y. Shin, W.K. Cha, S. Oh, N. Lee and J. Kim, *Materials Science and Engineering A*, 528 (2011) 3350-3357.
9. H.S. Lu, Y.H. Yang, G. Chen, X. Chen and X. Wang, *Procedia Engineering*, 130 (2015) 828 – 834
10. D. Belato, W. Rosado, D.D. Waele, D. Vanderschueren and S. Hertelé, *Sustainable Construction and Design*, 4 (2013), 1-10.
11. T.K. Lee, H. J. Kim, B.Y. Kang and S.K. Hwang, *ISIJ International*, 40 (2000), 12.
12. S.Y. Shin, B. Hwang, S. Lee, N.J. Kim and S.S Ahn, *Materials Science and Engineering A*, 458 (2007) 281-289.
13. ISO 6892-1:2009 specifies the method for tensile testing of metallic materials and defines the mechanical properties which can be determined at room temperature
14. ISO 5817:2014 Welding -- Fusion-welded joints in steel, nickel, titanium and their alloys (beam welding excluded) -- Quality levels for imperfections
15. EN 10045-2 Metallic materials. Charpy impact test. Part 2: Verification of the testing machine (pendulum impact)
16. EN 10045-1 Metallic materials. Charpy impact test. Part 1: Test method
17. J-H. Kim, S-W. Choi, D-H. Park and J-M Lee, *Materials and Design*, 65 (2015) 914–922
18. EN ISO 148-1:2009 Metallic materials - Charpy pendulum impact test - Part 1: Test method.
19. EN 10028-2: 2003 Flat products made of steels for pressure purposes – Part 2: Non – alloy and alloy steels with specified elevated temperature properties.